Fachtagung "Experimentelle Strömungsmechanik"
6.–8. September 2022, Ilmenau

Vorteile der bildgebenden Durchflusszytometrie für die analytische Bewertung einzelner Nanopartikel und Nanopartikelwolken anhand ihrer Brownschen Molekularbewegung

Opportunities of Brownian Motion Imaging Flow Cytometry for the Analytical Assessment of Individual Nanoparticles and Nanoparticle Collections

Julia Sophie Böke, Adewale Adejimi, Thomas Henkel
Leibniz Institute of Photonic Technologies, Albert-Einstein-Str. 9, 07745 Jena

Brownsche Bewegung, bildgebende Durchflusszytometrie, Dunkelfeld, Nanopartikel Analyse
Brownian motion, imaging flow cytometry, darkfield imaging, nanoparticle tracking analysis

Abstract

Brownian motion (BM) is a stochastic process that describes the random movement of suspended particles. The velocity distribution for an individual particle depends on the particle size, mass, and shape. In return, information on these particle properties can be derived from the measured velocity distribution of the BM. In our work, we utilize a flow cell, as known from imaging flow cytometry (IFC), to measure the BM characteristics of individual gold nanoparticles (NPs) under continuous flow conditions with darkfield transmission mode illumination. Challenges related to data recording and analysis under continuous flow conditions were highlighted, and approaches to overcoming them were discussed and demonstrated.

Introduction

Characterizing the size of nanoparticles (NPs) and understanding their diffusion properties is crucial to a variety of applications and research fields ranging from the quantification of molecular binding in biosensors to cell- and subcellular motion (Hole et al. 2013; Doorley and Payne 2011). The interaction of NPs with their environment depends on their size (Tenzer et al. 2011), which is relevant when NPs are used for applications in medicine as contrast agents (Tong et al. 2009). Observing NPs in suspension allows tracking of each particle's Brownian motion (BM) (Einstein 1905), enabling to determine the particle size distribution (Filipe et al. 2010).

The most commonly used imaging techniques to analysis and characterize NPs include liquid-cell (scanning) transmission electron microscopy (LC(S)TEM), nanoparticle tracking analysis (NTA) and dynamic light scattering (DLS). In contrast, DLS is considered rather user-friendly and time-efficient compared to the other techniques (Filipe et al. 2010). However, its tendency to detect small amounts of larger particles is a drawback when dealing with dust contamination or samples containing aggregates.

In this study, we analyze the BM of plasmonic gold NPs, diffusion coefficients and their hydrodynamic diameter under darkfield illumination in transmission mode. Commercially available

GALA e.V., Karlsruhe, Germany, ISBN 978-3-9816764-8-8

gold NPs with a nominal diameter of 250 nm are observed in a microfluidic chip in a stationary scenario and under constant flow utilizing imaging flow cytometry (IFC). Tracking data provides precise information on temporal changes of position, displacement, and velocity of the NPs. However, data is still superseded by the global velocity of the fluid element surrounding the particle. After compensation for the global fluid velocity, the BM trajectory is used to calculate the diffusion coefficient and the hydrodynamic diameter. Measurements are recorded for two cases, (a) stationary case, where the particles undergo BM without any external flow and (b) flow scenario, where particles are measured while continuously passing a flow cell for IFC.

In this study, we analyze the BM of plasmonic gold NPs having an average diameter of 250 nm under continuous flow conditions for measuring their diffusion coefficients and hydrodynamic diameter. Therefore, particle motion inside a flow cell was continuously imaged under dark field illumination at a high frame rate of 500 frames per second (fps). Data were recorded for continuous unidirectional flow and zero flow conditions and subjected to data analysis. Challenges in data analysis under continuous flow were highlighted, and approaches to overcoming them were discussed and demonstrated. As a side effect, the method qualifies for the measurement of flow fields with outstanding temporal and spatial resolution.

Materials and Methods

Microfluidic chip and fluid management

The microfluidic device was prepared using lithography and wet-etching on glass with an etch depth of 100 µm to create microfluidic half-channels. Afterwards, two microfluidic glass slides are bonded against each other.

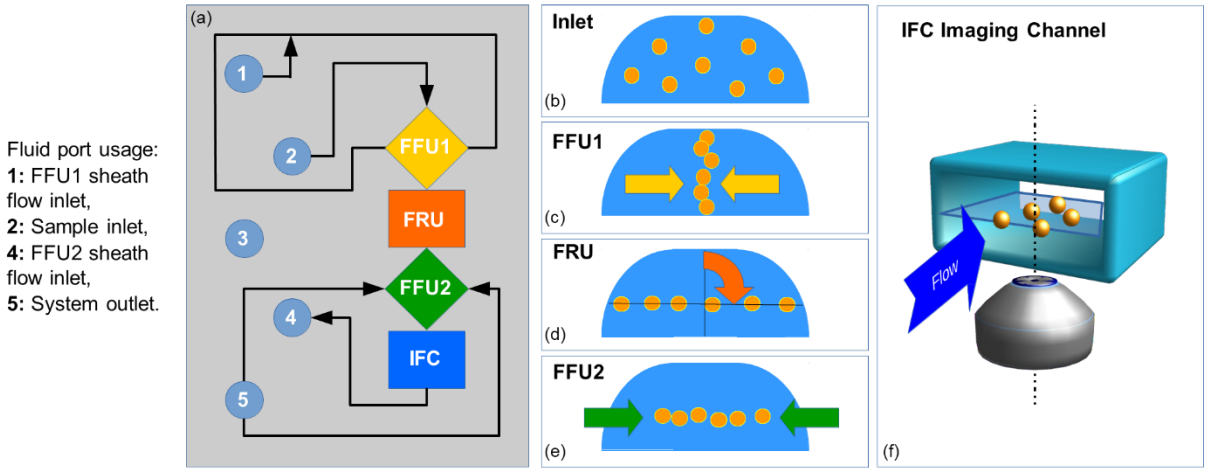

Fig. 1: Schematic drawing of the microfluidic device and its functional units (a). The particles fill the sample channel following port 2 (b). The sheath flow of FFU1 (arrows) focuses the sample lamella in the middle of the channel (c). The FRU rotates the sample stream by 90° (d). FFU2 focuses the sample stream away from the inner side walls (e). In the IFC unit, the particles arrive in the focal plane of the imaging setup (f).

The utilized microfluidic device for IFC implements a hydrodynamic flow focusing (Fig. **1**), which automatically aligns all particles, passing the flow cell within the focal plane of the imaging system (Kleiber et al. 2020). It is composed of a first flow-focusing unit (FFU1), shown in Fig. **1** (c), which laterally shrinks the particle-containing sample fluid into a vertical lamella, a flow rotation unit (FRU) which rotates the vertical lamella into a horizontal one (d), a second FFU which laterally moves particles away from near-wall positions (e) and a widened observation channel (width =480 µm, height =100 µm, length = 3050 µm) with planar bottom for image acquisition by video microscopy (f).

GALA e.V., Karlsruhe, Germany, ISBN 978-3-9816764-8-8

The fluids were controlled using three 500 µl syringes (ILS Innovative Laborsysteme GmbH, Stützerbach, Germany) fitted into a syringe pump (CETONI GmbH, Korbußen, Germany) and is connected to the microfluidic device via three PTFE-HPLC tubing with 0.5 mm inner diameter and controlled with neMESYS software. The syringe pump controls the input flow rates of the fluids. Input flow rates were chosen to create a particle flow velocity of 1 mm/s in the imaging region after the second flow-focusing unit. The flow rate settings were 0 nl/s for the stationary case and 16 nl/s, 2 nl/s and 4 nl/s for FFU1, sample and FFU2, respectively.

Darkfield microscope

The optical setup consists of a self-built upright darkfield microscope, equipped with a 10x long distance objective M-Plan Apo 10x/0.28, working distance (WD) 34 mm (Mitutoyo Corporation, Kawasaki, Japan), a 200 mm tube lens with tubus (Navitar Inc., Rochester, US). Dark field illumination was realized in transmission mode using an infinity beam Lumo Series L1W1MLT500s-20E white LED light source (Fulham Co. Inc., Hawthorne, USA) with a beam diameter of 21 mm, a dark field ring aperture plate with an outer diameter of 22.4 mm and an inner aperture diameter of 14 mm. The condenser lens system has a combined focal length of 16.65 mm and NA of 0.55. Images were recorded using a monochrome CMOS-camera acA1920-155 (Basler AG, Ahrensburg, Germany), with a pixel size of 5.86 µm² and sensor size of 1920x1200 pixels.

Sample and sample preparation

Suspended plasmonic gold NP with a nominal particle diameter of 250.0 ± 8.0 nm, at a concentration of 0.01% w/v (g/ml) in water (BBI Solutions OEM Ltd., Crumlin, UK) was used as stock. For measurements, 1.5 ml stock was diluted with 0.5 ml deionized (DI) water. Independent reference measurement of the particle size was performed using the LM 10 nanoparticle tracking analyzer (NanoSight Ltd., Malvern, UK), yielding a mean particle size of 191.0 nm with a standard error of 6.5187 nm.

Brownian Motion Imaging Flow Cytometry

For Brownian motion analysis, an IFC microfluidic chip (Fig. **1**) with an imaging channel height = 100 µm was mounted into the stage of the microscope and connected with the 500 µl syringes according to the following scheme: FFU1: DI water, FFU2: DI water, Sample: NP suspension, diluted in DI water. For the stationary (zero flow) measurement, the microfluidic chip was filled with diluted NP suspension, and the flow was stopped for the measurement. Image data was recorded for a reduced region of interest (ROI) of 1920x200 pixels at a frame rate of 500 fps and an exposure time of 30 µs. The measurement under flow conditions was performed with FFU1: 16 nl/s, Sample: 2 nl/s, and FFU2: 4 nl/s. After flow equilibration, 1000 image frames with a reduced ROI of 1920x200 pixels were recorded at a frame rate of 500 fps at 30 µs exposure time. Additionally, a blank reference image and a dark reference image were recorded at the same camera settings.

Results and Discussion

NPs sizes can be analysed by optical detection of their Brownian motion displacements and velocities. The velocities of these NPs decrease with increasing particle size since smaller particles diffuse faster than larger particles. The motivation behind this study is to characterise the accurate size of NPs, as this is essential because of their applications in the field of colloid chemistry. NPs are used as biosensors through binding of analytes where a change in size, hydrodynamic properties and spectral properties can be observed. Our method utilizes IFC, to

GALA e.V., Karlsruhe, Germany, ISBN 978-3-9816764-8-8

characterise the particle diameter based on its diffusion coefficient and hydrodynamic diameter of NPs. We present our results in three cases, firstly from a stationary measurement of NPs, where they are allowed to diffuse freely without any external manipulation, secondly by our new approach of flow cytometry, where we subject the confined particles to the desired flow rate. In all experiments, the image sequences were recorded at 500 fps, 30 µs exposure time.

During image acquisition, the particles pass through the flow cell in the xy-plane at half the height of the imaging channel. According to its dimension (w = 480 µm, h = 100 µm), this can be approximated as a capillary slit channel with a parabolic velocity distribution over the channel height, where the maximum velocity is at half-height given by Eq. 1. Eq. 2 yields the mean fluid velocity from the given flow rate Q and the channel cross-sectional area A.

$$U_{centre} = \frac{2}{3} \cdot U_{mean} \tag{1}$$

$$U_{mean} = \frac{Q}{A}(mm/s) \tag{2}$$

Due to the parabolic velocity distribution in z-direction, the velocity of the particles change with their z-position, affected by their Brownian motion. Hence, Brownian motion displacement and velocities can be measured best along the y-dimension of our domain.

Einstein-Stokes relation below provides the relation between diffusion coefficient D, and hydrodynamic diameter d, for a particle that experiences Brownian motion (Edward 1970)

$$D = \frac{K_B T}{3\pi\eta d} \tag{3}$$

where K_B is the Boltzmann constant, T the absolute temperature in K, η the dynamic viscosity of the liquid and d the particle diameter.

BM is a three-dimensional movement. The diffusion coefficient and hence the hydrodynamic diameter can be calculated from the mean squared displacement $\overline{(x,y,z)^2}$ of a single particle. The standard deviation, $\sigma^2_{x,y,z}$, of the motion relates to the diffusion coefficient by:

$$\sigma_{x,y,z}{}^2 = 2D \cdot t \tag{4}$$

Consequently, in image-based tracking of NPs, the dimensionality reduces. In the following, we will differentiate between two cases, stationary and continuous flow.

In the subsequent discussion, we assume that the particles are imaged in the xy-plane of a Cartesian coordinate system, with the z-axis parallel to the optical axis of the imaging system. The flow cells are mounted in the xy-plane with the fluid flowing in the x-direction.

The stationary case describes the movement of suspended NPs without an external force field or pressure gradient. Thus, particle movement is tracked along two dimensions (Hole, 2013). Hence, the mean-squared displacement reduces to

$$\overline{(x,y)^2} = \frac{4\,K_B T}{3\pi\eta d} \cdot t \tag{5}$$

Fig. 2 (a) shows a typical trajectory taken by a free diffusing single particle over the recording time. Fig. 2 (b) shows the intrinsic trajectory of a suspended NP tracked over the field of view.

GALA e.V., Karlsruhe, Germany, ISBN 978-3-9816764-8-8

For characterisation, we assume a uniform time step size and analyse the particle displacement between two subsequent time steps over time.

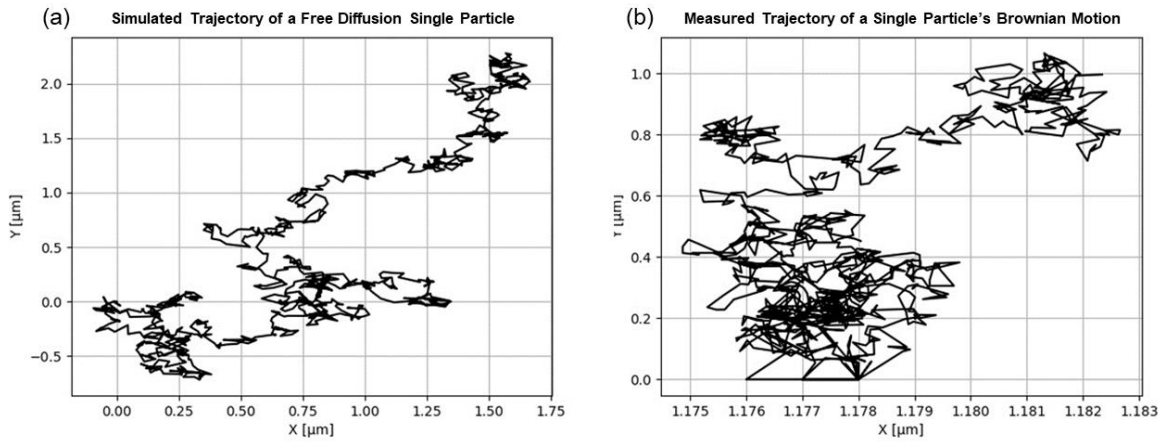

Fig. 2: Brownian motion of a particle in x and y. Simulation of a typical trajectory of a freely diffusing single particle (a). Exemplary trajectory of a tracked NP in suspension during a measurement (b).

In the stationary case, 1000 frames contain over 970,000 particle observations from which 592 single-particle tracks were reconstructed over at least 500 frames. Fig. 3 below shows the probability density of the mean displacement in y-direction for the whole particle cloud (a) and a single NP track (b) in stationary measurements. The histogram data of the mean displacement in y-direction fit with a normal distribution, having the same standard deviation as the particle distribution. The standard deviation was not independently calculated but calculated as the standard deviation of the observations. This fitting confirms BM.

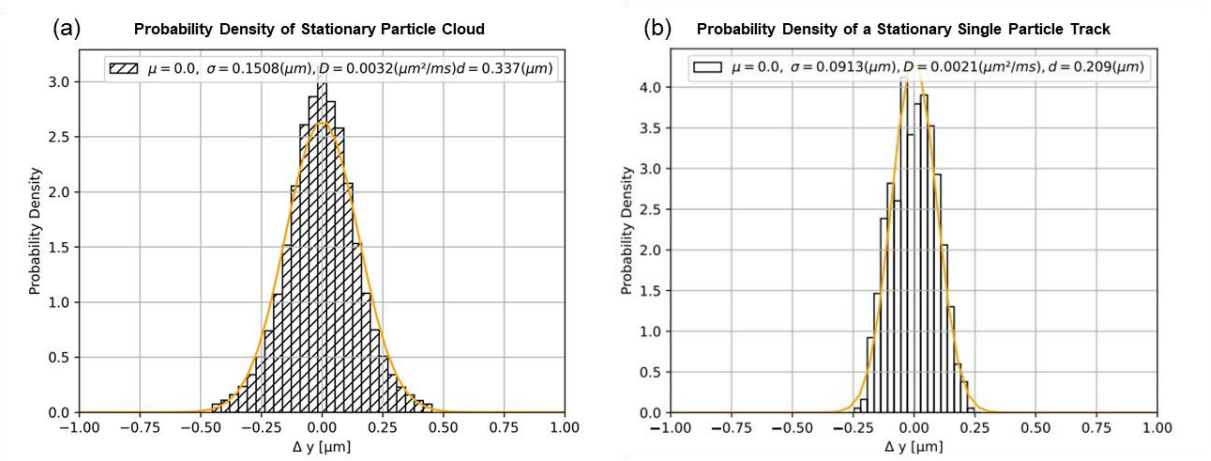

Fig. 3: Histogram distribution of the probability density of a stationary particle cloud with Gaussian of its standard deviation (= 0.1508 µm) (a) and exemplary single-track NP (ID = 159871) with a Gaussian of its standard deviation (= 0.0913 µm) (b).

The particle observations in Fig. 3 (a) show a standard deviation of their motion along the y-axis of 150.8 nm. Analysing our image data for the measurements in flow leads to a mean particle diameter of 337 ± 6.3 nm, calculated from the particle clouds over the recorded frames.

The BM of NPs under constant flow can be best quantified for the spatial component perpendicular to the flow direction within the focal plane. Conforming to the orientation of our coordinate system, this becomes the y-axis. For movement along the y-axis follows analogue from Eq. 4 (Hole et al. 2013):

GALA e.V., Karlsruhe, Germany, ISBN 978-3-9816764-8-8

$$\overline{(y)^2} = \frac{2\,K_B T}{3\pi\eta d} \cdot t \qquad (6)$$

For the flow-through case, 1000 frames containing approximately 140,000 particle observations were recorded. To ensure the applicability of statistical methods, only particle tracks with more than 150 observations were included, leading to 113 reconstructed single NP tracks. While observing the particles' Brownian motion in flow, we show approximately 20% of the captured and measured NP tracks in Fig. 4 (a). The BM is exemplarily shown in the zoomed-in region. Fig. 4 (b) illustrates the movement of a single-particle track. The interpolation refers to the trajectory of the fluid lamella, indicating a slight overall shift. Thus, the corrected trajectory refers to the single-particle trajectory corrected by the global drift within the fluid lamella.

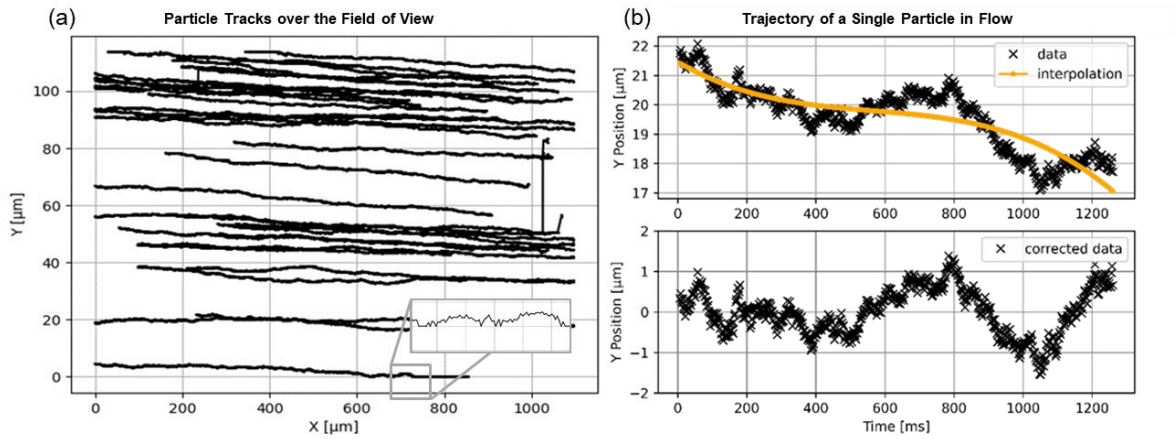

Fig. 4: Selected particle tracks with sub-pixel precision (a). Trajectories of a single particle in flow (b).

In Fig. 5 below, we show the probability density of the particles in flow. The histograms fit the Gaussian distribution, with the same standard deviation as the particle distribution, confirming BM. Fig. 5 (a) shows the probability density for the whole particle cloud in flow, and Fig. 5 (b) shows the probability density for a selected single particle track in flow.

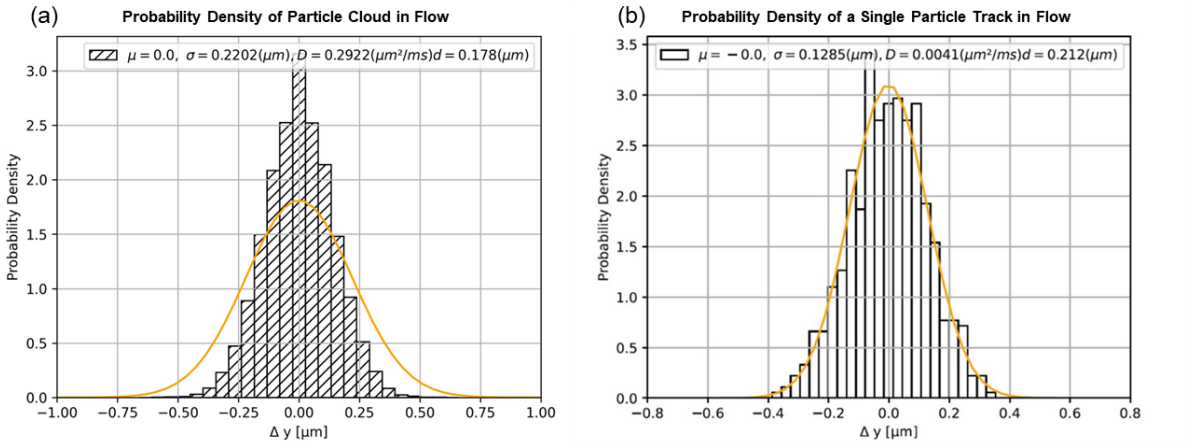

Fig. 5: Histogram distribution of NP cloud in flow fitted with a Gaussian of its standard deviation (σ_y^2 = 0.22 µm) (a). Histogram distribution of a single NP fitted with a Gaussian of σ_y^2= 0.13 µm (b).

The particle observations in Fig. 5 (a) show a standard deviation of their motion along the y-axis of 220.2 nm. Analysing our image data for the measurements in flow leads to a mean particle diameter of 178 ± 4.5 nm, calculated from the particle clouds over the recorded frames. The probability density histogram shows a disproportionate number of particles with little to no movement. Those observations could result from background artifacts, which skew the

GALA e.V., Karlsruhe, Germany, ISBN 978-3-9816764-8-8

calculations of the hydrodynamic diameter from the particle cloud. The deviation in diameter for a selected single-particle observation results in a particle diameter of 212 nm, in Fig. 5 (b).

Up until now, the fluid trajectory was directly derived from the respective track by averaging positions. However, this averaging is not statistically exact since the number of averaged positions is limited. Alternatively, a flow field of the complete domain could be obtained, which is averaging all observed velocities of all particles over time, as illustrated in Fig. 6 for the single-particle observation shown in Fig. 4 (b).

The flow field was obtained as an interpolation $u_x, u_y(x, y, t)$ using a radial basis function (RBF) based interpolator with a linear kernel model with smoothing activated. Fig. 6 below shows the fluid flow field at the time when the track passed the flow field. The particle (ID= 17315) arrives at t = 240 ms and leaves at t = 1440 ms. Therefore, the flow field was plotted for t = 1000 ms.

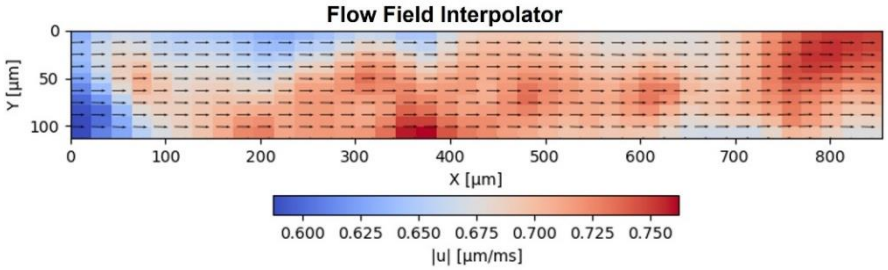

Fig. 6: Exemplary flow field at the time, t = 1000 ms, for a chosen particle observation.

In Fig. 7 (a), we show the selected particle's positions within the region of interest. Fig. 7 (b) and (c) show the x and y components of the particle velocity and the fluid trajectories obtained from the interpolation model.

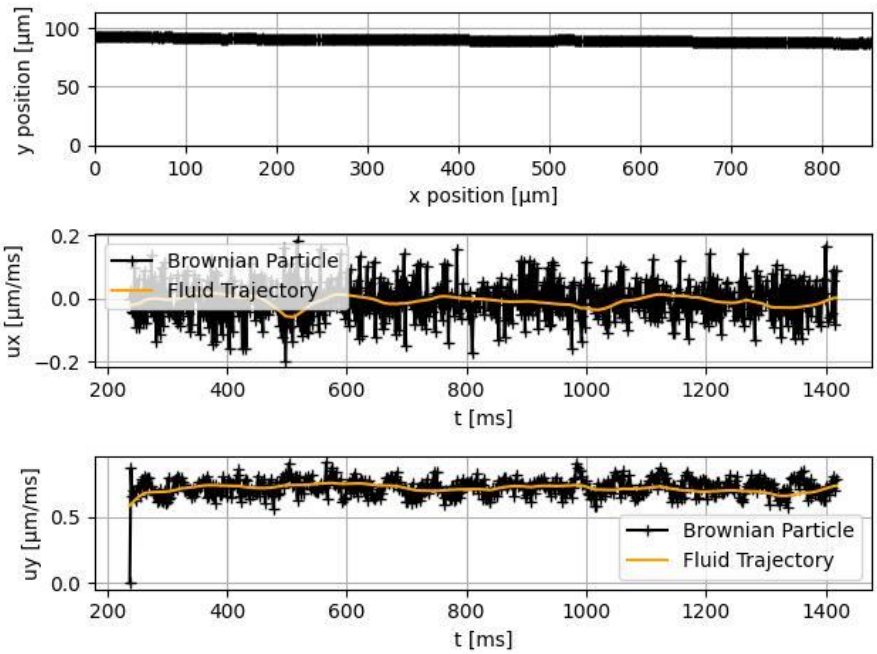

Fig. 7: Particle Positions within the region of interest (a). Particle velocity components in x (b). Particle velocity components in y (c).

GALA e.V., Karlsruhe, Germany, ISBN 978-3-9816764-8-8

Conclusion

IFC can be used to analyse and characterize NPs based on their Brownian motion. We imaged NPs both under stationary and continuous flow conditions, tracked particle observations on a single particle level over the field of view and quantified their movement as well as their hydrodynamic diameter. For the stationary scenario, we calculate a mean diameter of 337 ± 6.3 nm from over 592 single-particle tracks over at least 500 frames. For the continuous flow scenario, we reconstructed 113 NP tracks of at least 150 particle observations leading to a calculated mean diameter of 178 ± 4.5 nm. Both diameters are in the same order of magnitude as the reference measurement performed with the NanoSight of 191.0 ± 6.5 nm. While parameters still need to be optimized, the first results of Brownian motion IFC presented here are promising. We differentiated Brownian motion from the global fluid trajectory. The NP tracking data can also be used to analyse and study the flow profile for different fluid parameter settings.

Acknowledgment

This project has received funding from the European Union's Framework Programme for Research and Innovation Horizon 2020 under the Marie Sklodowska-Curie Grant Agreement No. 860775. The authors acknowledge funding of this work by funds of the Germans Government's Special Purpose Fund held at Landwirtschafliche Rentenbank during the project MIPOS (FKZ 924493). The authors gratefully acknowledge the funding of this work by the German Federal Ministry of Education and Research within the funding program “Photonics Research Germany” during the Project SARSCoV2Dx, Funding Signature 13N1572.

Literature

Doorley, G.W., Payne, C.K., 2011: "Cellular Binding of Nanoparticles in the Presence of Serum Proteins". *Biophysical Journal* 100 (3), 317a.

Edward, J.T., 1970: "Molecular volumes and the Stokes-Einstein equation". *J. Chem. Educ.* 47 (4), p. 261.

Einstein, A., 1905: "Über die von der molekularkinetischen Theorie der Wärme geforderte Bewegung von in ruhenden Flüssigkeiten suspendierten Teilchen". *Annalen der Physik* vol. 4, t. 17.

Filipe, V., Hawe, A., Jiskoot, W., 2010: "Critical evaluation of Nanoparticle Tracking Analysis (NTA) by NanoSight for the measurement of nanoparticles and protein aggregates". *Pharm Res* 27 (5), pp. 796–810.

Hole, P., Sillence, K., Hannell, C., Maguire, C.M., Roesslein, M., Suarez, G. et al., 2013: "Interlaboratory comparison of size measurements on nanoparticles using nanoparticle tracking analysis (NTA)". *J Nanopart Res* 15 (12), p. 2101.

Kleiber, A., Ramoji, A., Mayer, G., Neugebauer, U., Popp, J., Henkel, T., 2020: "3-Step flow focusing enables multidirectional imaging of bioparticles for imaging flow cytometry". *Lab on a chip* 20 (9), pp. 1676–1686.

Tenzer, S., Docter, D., Rosfa, S., Wlodarski, A., Kuharev, J., Rekik, A., et al., 2011: "Nanoparticle size is a critical physicochemical determinant of the human blood plasma corona: a comprehensive quantitative proteomic analysis". *ACS nano* 5 (9), pp. 7155–7167.

Tong, L., Wei, Q., Wei, A., Cheng, J.-X., 2009: "Gold nanorods as contrast agents for biological imaging: optical properties, surface conjugation and photothermal effects". *Photochemistry and Photobiology* 85 (1), pp. 21–32.

GALA e.V., Karlsruhe, Germany, ISBN 978-3-9816764-8-8